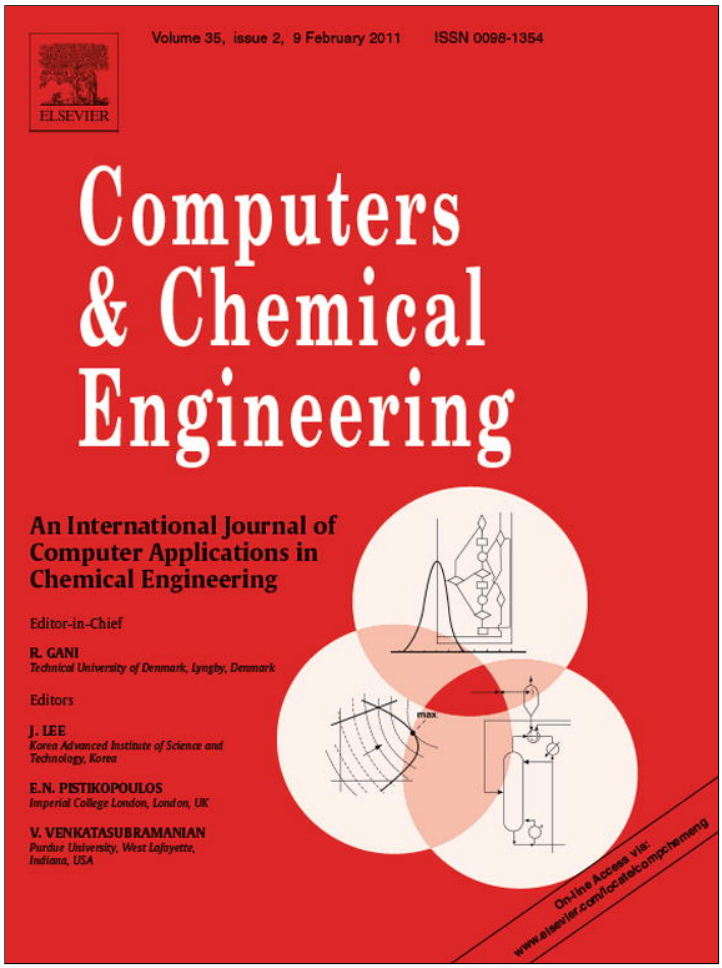

Computers and Chemical Engineering 35 (2011) 356–371

Contents lists available at ScienceDirect

Computers and Chemical Engineering

journal homepage: www.elsevier.com/locate/compchemeng

Petri-net models for comprehensive hazard analysis of MOCVD processes

Li-Ping Chung, Chuei-Tin Chang*

Department of Chemical Engineering, National Cheng Kung University, 1 Ta-Hsueh Road, Tainan 70101, Taiwan, ROC

ARTICLE INFO

Article history:
Received 25 May 2009
Received in revised form 8 May 2010
Accepted 10 May 2010
Available online 19 May 2010

Keywords:
MOCVD
Adsorption
Safety
Petri-net model
Simulation

ABSTRACT

Reducing contamination level is of primary importance for the safety and efficiency of a MOCVD process. Off-line fault identification is one of the basic tasks that must be performed in hazard analysis to identify potential operational problems. For illustration convenience, the scope of present study is limited to the purge-gas purifier of the process. A systematic step-by-step procedure is proposed in this paper to construct Petri nets for modeling the purification system. Efficient hazard assessment studies have been performed by simulating the fault propagation behaviors on the basis of the system model. A comprehensive list of possible fault origins has been thoroughly examined to demonstrate the effectiveness of the proposed approach.

1. Introduction

Metal Organic Chemical Vapor Deposition (MOCVD) is a form of CVD operation which utilizes metal organic compounds as its precursors. There are several excellent review articles and also books that go into depth on this complex subject (Stringfellow, 1989; Stringfellow, 1994, chap. 12; Thompson, 1997). As a general rule, cleanliness is essential in any semiconductor manufacturing process. The link between the unwanted impurities in process gases and device quality is well established (Newey, 2001). Reducing contamination level is of primary importance for the highly sensitive MOCVD processes, as incorporation of impurities into epilayers, even at trace levels, may result in unintentional doping, lattice defects and/or other undesirable effects (Sangwal, 1996; Veintemillas-Verdaguer, 1996; Watanabe et al., 2003). Furthermore, the hydride gases used in MOCVD operation are often highly toxic, and most of the metal organics are pyrophoric (Jones & O'Brien, 1996). For example, trimethylindium (TMI) may react violently with air, water, compounds containing active hydrogen such as alcohols and acids, and also those containing oxygen or organic halide. Such impurities must be thoroughly removed from the process gases with purifiers. Therefore, it is clear that there are significant safety risks associated with the transportation, storage and use of the process materials in the MOCVD operation.

To identify potential operational problems, off-line fault identification is one of the basic tasks that can be performed in designing or revamping any industrial process. Numerous techniques are available for this purpose, e.g., fault-tree analysis (FTA), event tree analysis (ETA), failure modes and effects analysis (FMEA) and hazard and operability study (HAZOP). In implementing these methods, there are always needs (1) to reason deductively for finding all combinations of basic events that could lead to an undesirable condition and/or (2) to predict all possible consequences of a given fault origin. However, if every fault propagation mechanism is to be identified manually, a rigorous analysis is bound to be labor- and time-consuming and its results often error-prone. To alleviate these practical problems, there have been many attempts in the past to develop computer aids on the basis of various qualitative models. In the last two decades, the research on automatic hazard analysis has advanced significantly. Many efficient tools have already been adopted to develop the fault-tree synthesis algorithms, e.g., digraph (Chang & Hwang, 1992; Lapp & Powers, 1977), decision table (Kumamoto & Henley, 1979) and mini-fault tree (Kelly & Lees, 1986a, 1986b). Several generic expert systems have also been constructed to produce comprehensive HAZOP reports (McCoy, Wakeman, Larkin, Jefferson, et al., 1999; McCoy, Wakeman, Larkin, Chung, Rushton, & Lees, 1999; McCoy, Wakeman, Larkin, Chung, Rushton, Lees, & Heino, 1999; McCoy et al., 2000a, 2000b; Rossing, Lind, Jensen, & Jorgensen, 2010; Vaidhyanathan & Venkatasubramanian, 1996a, 1996b). The prerequisite for identifying the fault propagation mechanisms in implementing any of these methods is basically a qualitative system model. It can be observed from the literature that the digraph is by far the most popular choice (Allen & Rao, 1980; Andrews & Morgan, 1986; Chang, Hsu, & Hwang, 1994; Chang & Hwang, 1994; Vaidhyanathan & Venkatasubramanian, 1995). Although the

* Corresponding author. Tel.: +886 6 275 7575x62663; fax: +886 6 234 4496.
E-mail address: ctchang@mail.ncku.edu.tw (C.-T. Chang).

0098-1354/$ – see front matter © 2010 Elsevier Ltd. All rights reserved.
doi:10.1016/j.compchemeng.2010.05.006

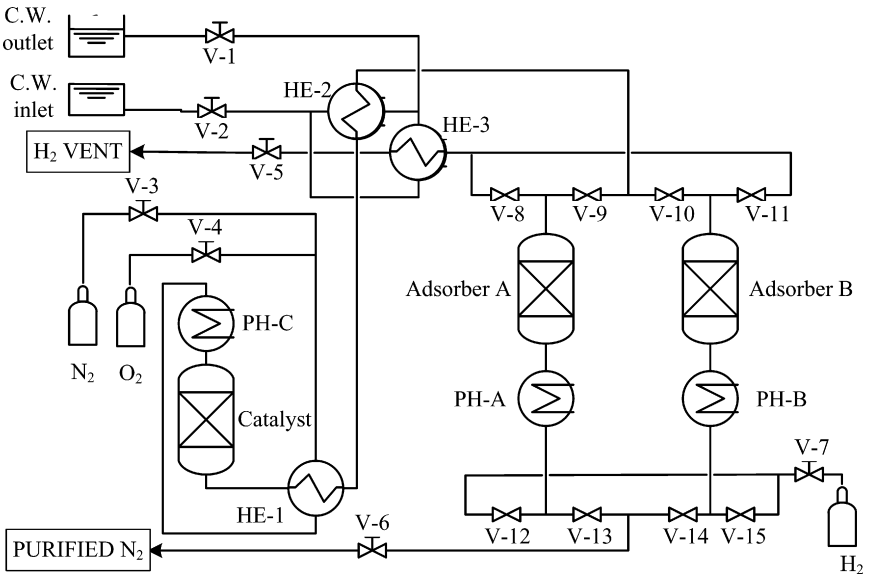

Fig. 1. Flow diagram of nitrogen purifier.

digraph-based approach has been proven to be useful, it is effective only in applications concerning the *continuous* processes. This is due to the fact that the digraph is inherently unsuitable for describing the dynamic causal relationships among time, discrete events, equipment states and system configurations in *sequential* operations, which is the dominant feature of the semiconductor manufacturing processes.

In the present work, the Petri net (Petri, 1962) is used as a modeling tool to circumvent the above-mentioned drawbacks. Notice that the previous applications of Petri net in hazard analysis were directed to the batch or semi-batch *chemical* processes. The idea of automating *procedure HAZOP* on the basis of Petri-net-digraph hybrid models was proposed by Srinivasan and Venkatasubramanian (1998a, 1998b). Szucs, Gerzson, and Hangos (1998) used the colored Petri nets to concisely represent the transient behaviors of the states, inputs and outputs in batch processes for fault diagnosis purpose. Balasubramanian, Chang, and Wang (2002) proposed a systematic approach to construct a generic Petri-net model for analyzing the fault propagation mechanisms in the liquid ammonia loading process. Wang, Wu, and Chang (2002) and Wang and Chang (2003, 2004) employed timed hybrid Petri nets to develop a systematic procedure for automatic hazard analysis of the sequential operations. They also developed deductive reasoning algorithms for fault identification in batch chemical processes. Zhao, Bushan, and Venkatasubramanian (2005a, 2005b) built efficient software tools for performing HAZOP analysis automatically. On the other hand, it should be noted that a large number of studies can also be found in the literature concerning the development of Petri-net models for the non-continuous sequential semiconductor processes. Cavalieri, Mirabella, and Marroccia (1997) described a scheduling approach for flexible semiconductor manufacturing systems based on colored Petri nets. They employed a heuristic algorithm to construct the reachability tree in order to find a low-cost schedule. Kim and Desrochers (1997) proposed a method for automatically structuring a Petri-net model of the semiconductor manufacturing procedures and suggested how the performance measures such as the capacity, on-line turn-around time, and work in process can be determined.

The objective of the present research is to modify/extend the aforementioned existing Petri net based hazard identification strategy to a special class of semiconductor processes, i.e., MOCVD. To facilitate detailed illustration, the scope of this paper is limited to the purifiers of process gases only. A more comprehensive study of the entire system will be carried out in the future. Notice that the ultra-pure nitrogen and hydrogen are used respectively as the purge gas and carrier gas for the metal organic precursors in the MOCVD process. The contamination control operations for such gases are essential for satisfactory wafer growth. In addition, removal of oxygen and moisture from these streams is also necessary for reducing the risk of fire hazards.

The remainder of this paper is organized as follows. The process flow diagram of a nitrogen purifier and its operating procedure (specified in the form of a Grafchart) are first presented in Section 2. The component models of all equipments in the purification system are also explained in detail next. The fault propagation mechanisms are outlined in Section 4. The model-building techniques for incorporating the failure mechanisms into the component models are discussed in the next section. Finally, the results of a comprehensive hazard analysis are presented at the end of this paper to demonstrate the effectiveness of the proposed approach.

2. Nitrogen purifier in MOCVD process

A reliable supply of ultra-high purity gas is one of the most critical requirements for running semiconductor plants. The flow diagram of a typical nitrogen purifier in MOCVD process is given in Fig. 1. This purifier consists basically of three types of operation units: the catalytic oxidizer, the adsorbers and the heat exchangers. With a proprietary catalyst to oxidize methane in nitrogen stream at 300 °C and an adsorbent to remove the other impurities (including the oxidized products of the catalytic bed), e.g., CO_2 and H_2O, at room temperature, a steady flow of sub-ppb nitrogen can be produced to satisfy the process needs. The oxidizer is equipped with a pre-heater (PH-C) to maintain the reaction temperature and a metering system to control oxygen flow precisely. The heat exchanger HE1 and cooler HE2 are used to lower the temperature of its exit gas before entering the adsorbers. Two adsorption columns (A and B) are operated alternately to remove traces of O_2, CO, CO_2, H_2 and H_2O remained in the nitrogen stream at room temperature. The saturated adsorbent is regenerated with hydrogen at elevated temperature and then cooled with the same gas. Again two pre-heaters (PH-A and PH-B) are installed to raise the inlet hydrogen temperature for regeneration purpose. The spent hydrogen is

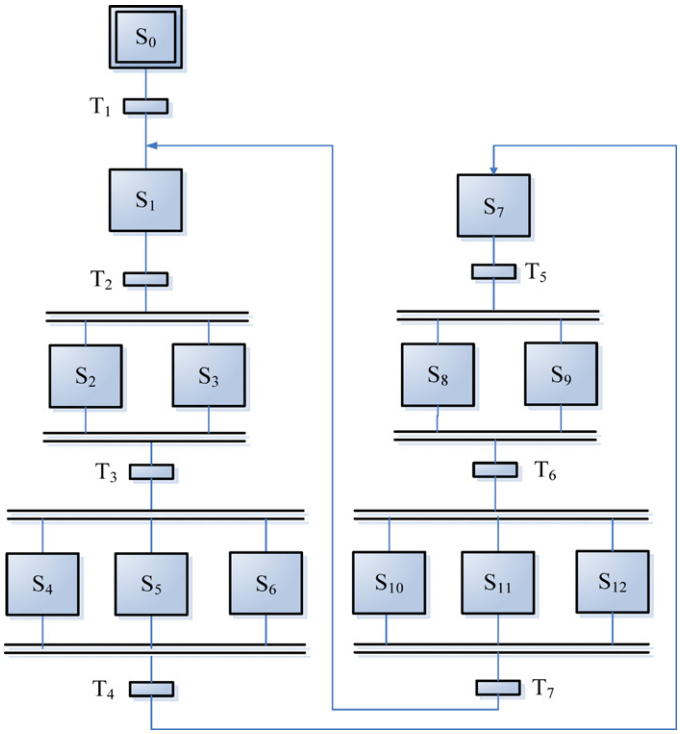

Fig. 2. Grafchart of purifier operating procedure.

cooled in HE3 and then vented. A continuous cooling-water supply is available for operating the coolers HE2 and HE3.

The required purification function can be performed by manipulating the valves V1–V15. The recipe for a complete operation cycle can be expressed with the Grafchart presented in Fig. 2. Notice that this Grafchart consists of 13 macro-operation steps which are marked by squares, i.e., S_0–S_{12}, and 7 transitions which are represented with bars, i.e., T_1–T_7. The specific operation actions to be carried out in each macro-step are specified in Table 1. Every transition in the Grafchart is associated with a set of conditions. These conditions are listed in Table 2. When all the conditions of a particular transition are satisfied, its preceding steps are terminated and then the succeeding steps activated. The activation conditions of transitions T_1, T_2, T_4, T_5 and T_7 are the initiation times of their succeeding steps, while those of T_3 and T_6 are valve positions. Notice that the execution times specified in this

Table 1
Operation steps of purifier.

Macro-steps	Specific step(s)
S_0	Initial steps[a]
S_1	Turn off PH-B
S_2	Close V9, open V12
S_3	Open V10, close V15
S_4	Open V8, close V13
S_5	Close V11, open V14
S_6	Turn on PH-A
S_7	Turn off PH-A
S_8	Close V8, open V13
S_9	Open V11, close V14
S_{10}	Open V9, close V12
S_{11}	Close V10, open V15
S_{12}	Turn on PH-B

[a] Initial conditions: C.W. system: V1(+) and V2(+); GAS supply system: V3(+), V4(+), V5(+), V6(+), V7(+), V8(−), V9(+), V10(−), V11(+), V12(−), V13(+), V14(−), and V15(+); adsorbers: T-A(1), T-B(2), SAT-A(0), and SAT-B(2); pre-heaters: PH-A(−), PH-B(+), and PH-C(+).

Table 2
Activation conditions in Grafchart.

Symbol	Activation condition(s)
T_1	$t = t_1$
T_2	$t = t_2, t_6, t_{10}, \ldots$
T_3	V10(+), V15(−), V12(+), V9(−)
T_4	$t = t_3, t_7, t_{11}, \ldots$
T_5	$t = t_4, t_8, t_{12}, \ldots$
T_6	V8(−),V13(+), V11(+), V14(−)
T_7	$t = t_5, t_9, t_{13}, \ldots$

Grafchart are arranged sequentially, i.e., $t_1 < t_2 < t_3 < \cdots$. Also, the symbol "+" is used to denote that the corresponding valve position is "open" or pre-heater power is "on", and the symbol "−" means otherwise.

3. Component models

It can be observed from Fig. 1 that the purifier system consists of many different components, i.e., 15 valves (V1–V15), 3 pre-heaters (PH-A, PH-B and PH-C), 3 heat exchanges (HE1, HE2 and HE3), 1 catalytic oxidization column, and 2 adsorption columns (adsorber A and adsorber B). These components can be classified into a hierarchy of four different levels (Wang & Chang, 2003):

- Level 1: controller (i.e., PLC);
- Level 2: actuators (i.e., valves and heating elements);
- Level 3: process units (i.e., heat exchangers, adsorbers and reactor);
- Level 4: sensors.

Basically every hardware item in the P&ID can be described with a component Petri-net model. Each component consists of two distinct parts. One is used to characterize the equipment state and the other the input–output conditions. In general, the state of a component may be switched from one to another during different phases/periods of normal operation. The Petri nets are used to mimic these transition processes. For completeness, a brief review of the ordinary Petri net and its extensions is provided in Appendix A. Following are detail descriptions of the component models adopted in the present study:

3.1. Programmable logic controller

The operation steps specified in a recipe can be executed with a programmable logic controller (PLC). The control signals issued by a PLC usually create changes in the equipment states of valves and pre-heaters through actuating devices. The controller in the purification system can be described with the Petri net given in Fig. 3. In this model, four discrete places, i.e., P1–P4, are used to respectively represent the four different controller states and each is associated with a distinct period (or phase) in an operation cycle, i.e., periods 1–4. The duration of each time period is stipulated as a time delay (T) on the output transition of the corresponding place. Notice that a set of sequential and/or concurrent operation steps are prescribed within the dotted line in Fig. 3 according to the Grafchart given in Fig. 2. Places S_1–S_{12} here represent the corresponding macro-operation steps specified in Table 1. Every such place is further connected to a non-timed transition with a static test arc, and then to places denoting the commands for specific control actions. Since these actions are taken to alter the equipment states of designated valves and/or pre-heaters in the purifier system, these changes should be viewed as the necessary conditions for completing the given macro-step.

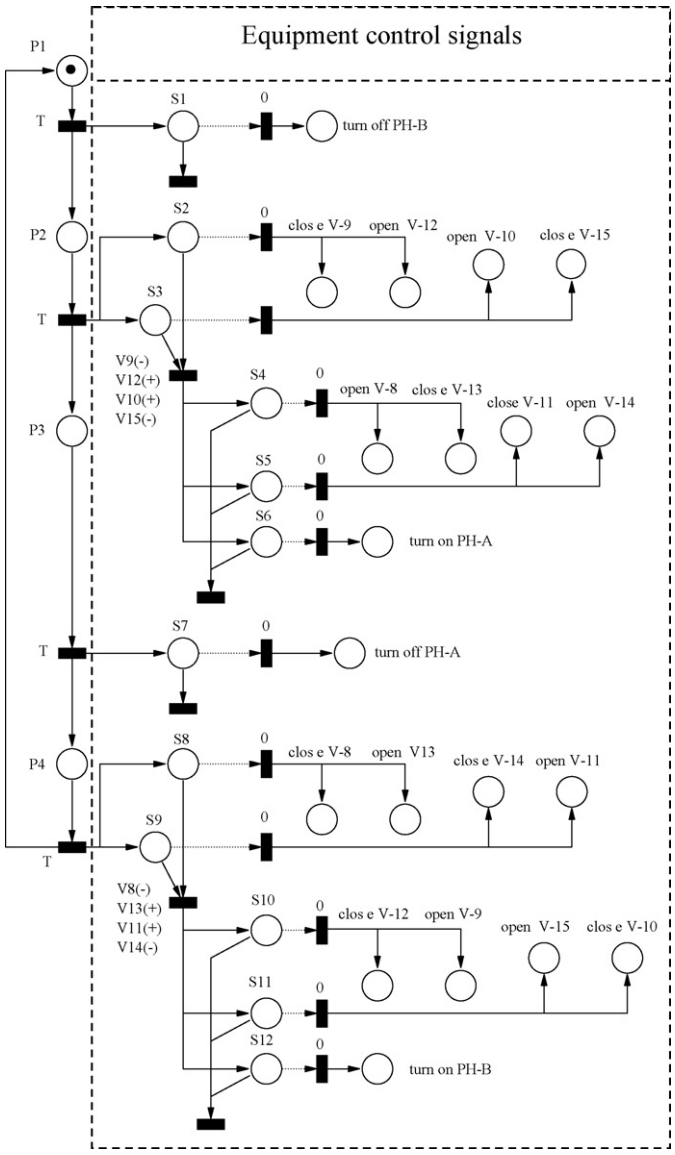

Fig. 3. Petri-net model for PLC.

Thus, other than the places for the specific operation commands, each of the places associated with the macro-steps S_1–S_{12} is connected by a normal arc to an additional output transition denoting the step-completion event and, in addition, the places reflecting the completion conditions are also linked to this transition with test arcs.

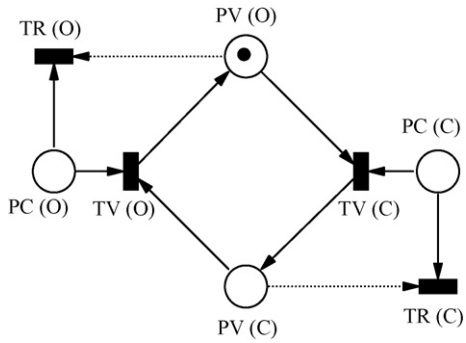

Fig. 4. Valve/pre-heater model.

3.2. Valves and pre-heaters

Only two alternative states are needed for characterizing a valve or pre-heater in normal operation. A standard Petri net is thus used in this work for describing the transition processes between these two states. This model is presented in Fig. 4. Let us consider a valve as an example. The places PV(O) and PV(C) denote respectively the two opposite positions of valve, i.e., open and close. The transitions TV(O) and TV(C) represent the valve-switching actions from PV(C) to PV(O) and vice versa. Notice that the input place PC(O) of the transitions TV(O) can be interpreted as the valve-opening command from PLC. Similarly, the place PC(C) can be considered as the control command for valve-closing action. Since it is possible to cause a material-transfer action when the corresponding valve is already open, transition TR(O) is introduced as the output of both PC(O) and PV(O) in this model. A normal arc is adopted in the former case to avoid a token being permanently kept in place PC(O), while a test arc is used in the latter to prevent loss of the tokens in PV(O). Finally notice that the transition TR (C) is adopted for the same reason.

The Petri net presented in Fig. 4 is also used to model the pre-heaters. In this case, the places PV(O) and PV(C) represent two opposite states, i.e., on and off, of a pre-heater respectively. The transitions TV(O) and TV(C) can be interpreted as the operation steps to turn the power of this component on and off respectively.

3.3. Adsorbers

The adsorption columns are the most important units in the purification process. At any time during normal operation, nitrogen flows through one of them and hydrogen the other. The former column is used for removing impurities and the latter is under preparation (regeneration and cooling) for the adsorption operation in later periods. The roles of these two columns are switched as soon as the one in service reaches saturation level. In this work, two variables, i.e., the *degree of saturation* and *temperature* of the adsor-

Table 3
Operation cycles of adsorption columns.

Time period	Operation modes		State transition processes	
	Adsorber A	Adsorber B	Adsorber A	Adsorber B
1	Adsorption	Regeneration	T-A(1) → T-A(1) SAT-A(0) + T-A(1) → SAT-A(1)	T-B(1) → T-B(2) SAT-B(2) + T-B(2) → SAT-B(0)
2	Adsorption	Cooling	T-A(1) → T-A(1) SAT-A(1) + T-A(1) → SAT-A(2)	T-B(2) → T-B(1) SAT-B(0) → SAT-B(0)
3	Regeneration	Adsorption	T-A(1) → T-A(2) SAT-A(2) + T-A(2) → SAT-A(0)	T-B(1) → T-B(1) SAT-B(0) + T-B(1) → SAT-B(1)
4	Cooling	Adsorption	T-A(2) → T-A(1) SAT-A(0) → SAT-A(0)	T-B(1) → T-B(1) SAT-B(1) + T-B(1) → SAT-B(2)

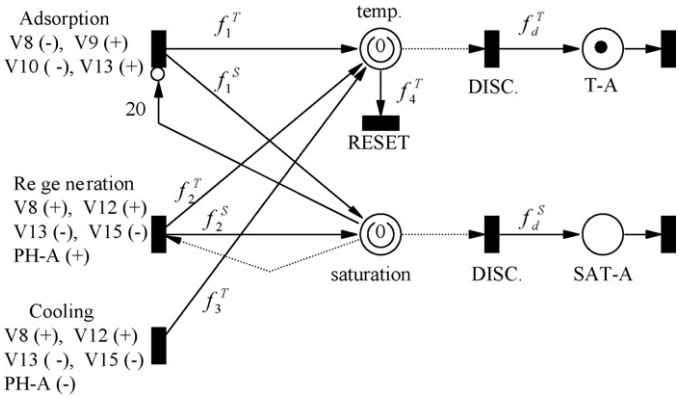

Fig. 5. Petri-net model for adsorber A.

bent, are adopted to characterize the equipment states of these two columns. For convenience, each state variable is discretized into three levels, i.e., 0, 1 and 2, denoting respectively the qualitative values of low, medium and high. A low level (i.e., 0) of saturation is achieved after regeneration. The saturation level 1 can be reached after one period of adsorption operation and, after two periods, the adsorbent is assumed to be fully saturated to level 2. On the other hand, the temperature level 0 is associated with an equipment condition which is unsuitable for adsorption; level 1 denotes atmospheric temperature; level 2 is the regeneration temperature. Consequently, a full operation cycle can be divided into four time periods. The operation modes of the two adsorbers in each period and the corresponding state transition processes are listed in Table 3.

The Petri-net model of column A is shown in Fig. 5. The token numbers in the discrete places T-A and SAT-A on the right are used to respectively represent the current temperature and saturation level of adsorber A. The transitions on the left are associated with the three distinct operation modes, i.e., adsorption, regeneration and cooling. Notice that, since each operation mode can be activated only by manipulating a set of valves and, in some cases, the pre-heater also to reach their designated states, these preconditions are listed next to the corresponding transition. As described in the previous section, the equipment states of valves and pre-heaters can be represented with discrete places in their respective Petri-net models. The implied causal relations can thus be realized by connecting such places and the above three transitions with static test arcs.

In a sense, the proposed adsorber model given in Fig. 5 can be viewed as a *qualitative evaluation mechanism* of the temperature and saturation level of the absorbent. The token numbers in the continuous places "temp" and "saturation" in this model represent respectively the qualitative measures of these two variables. The former (denoted as $\langle \text{temp} \rangle$) can be interpreted as the degree of deviation from a reference temperature and $-10 \le \langle \text{temp} \rangle \le +10$. The latter (denoted as $\langle \text{sat} \rangle$) is treated as a qualitative index of the accumulated mass of adsorbed impurities and $-10 \le \langle \text{sat} \rangle \le +10$. The discretized temperature and saturation level can then be determined from such measures according to the following weight functions:

$$f_d^T = 1 + \frac{\langle \text{temp} \rangle}{T_{\text{ref}}} \tag{1}$$

$$f_d^S = \frac{\langle \text{sat} \rangle}{S_{\text{ref}}} \tag{2}$$

where T_{ref} and S_{ref} denote respectively the qualitative measures of the reference temperature and saturation level. In this study, both values are set to 10. On the other hand, it can also be observed from Fig. 5 that the transitions representing the operation modes are connected to the continuous places "temp" and "saturation" with normal arcs. The qualitative evaluation procedures are implemented according to the weight functions f_i^T $(i = 1, 2, 3, 4)$ and f_j^S $(j = 1, 2)$ on these arcs. In this study, it is assumed that temperature equilibrium between the adsorbent and the incoming gas is reached immediately in the beginning of each operation period. Thus, the corresponding weight functions can be expressed as

$$f_1^T = (\langle \text{TN} \rangle - T_{\text{ref}}) \left(\frac{\langle \text{FN} \rangle}{\text{FN}_{\text{ref}}} \right) \tag{3}$$

$$f_2^T = f_3^T = (\langle \text{TH} \rangle - T_{\text{ref}}) \left(\frac{\langle \text{FH} \rangle}{\text{FH}_{\text{ref}}} \right) \tag{4}$$

$$f_4^T = \langle \text{temp} \rangle \tag{5}$$

where $\langle \text{TN} \rangle$ and $\langle \text{TH} \rangle$ denote respectively the qualitative measures of the temperatures of the nitrogen and hydrogen at the inlet of absorber; $\langle \text{FN} \rangle$ and $\langle \text{FH} \rangle$ represent respectively the qualitative measures of the nitrogen and hydrogen flow rates; FN_{ref} and FH_{ref} are the corresponding reference flow rates. Notice that the values of $\langle \text{TN} \rangle$, $\langle \text{TH} \rangle$, $\langle \text{FN} \rangle$ and $\langle \text{FH} \rangle$ are the token numbers of the corresponding continuous places in the input–output model described later. Notice also that the normal arc between place "temp" and transition "RESET" (with weight f_4^T) is meant to keep the token number in "temp" constant if the weights f_i^T $(i = 1, 2, 3)$ remain unchanged.

The weight functions used to determine the rates of increase and decrease in saturation level can be formulated respectively as

$$f_1^S = \left(\frac{\langle \text{C2N} \rangle}{\text{C2N}_{\text{ref}}} \right) \left(\frac{\langle \text{FN} \rangle}{\text{FN}_{\text{ref}}} \right) (2 - \langle \text{T-A} \rangle) \langle \text{T-A} \rangle \tag{6}$$

$$f_2^S = \left(\frac{\langle \text{FH} \rangle}{\text{FH}_{\text{ref}}} \right) (1 - \langle \text{T-A} \rangle) \langle \text{T-A} \rangle \tag{7}$$

where $\langle \text{C2N} \rangle$ and C2N_{ref} denote respectively the qualitative measures of the impurity concentration in the nitrogen stream and its reference value at the inlet of absorber; $\langle \text{T-A} \rangle$ is the token number of the discrete place "T-A".

Finally, notice that a delay time $\Delta\theta$ is assigned to every transition in this model. For simulation's convenience, such time delays are set to be one tenth of the length of each time period in an operation cycle.

3.4. Other components

It is assumed that the equipment states of others components in the purifier, i.e., the heat exchangers and the catalytic reactor, remain unchanged during normal operation. Consequently, the cause-and-effect relations between input and output conditions of every such single-state component are also fixed.

4. Fault propagation patterns

To facilitate the execution of a particular operation mode, every process fluid, i.e., nitrogen, hydrogen, oxygen and cooling water, must be transported along a distinct route in the pipeline network. These different material-transfer paths are altered from period to period by opening/closing a specific set of valves with the PLC. Obviously, it is imperative to produce an accurate and updated route map after the valve-switching steps are completed. This map is expressed with a path model in the present study. The effects of fault propagation can then be determined accordingly on the basis

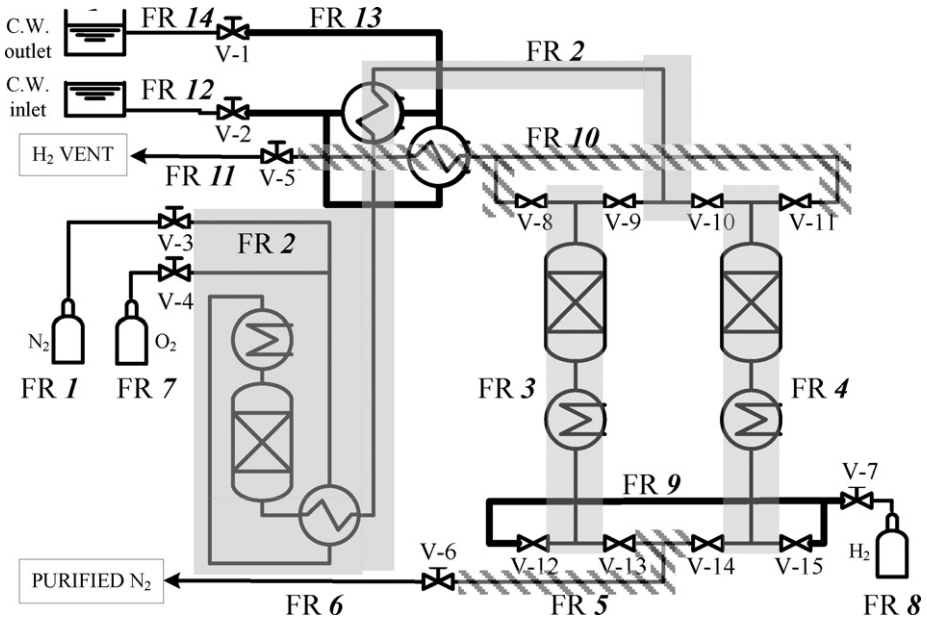

Fig. 6. Piping fragments.

of the input–output models of the components on the material-transfer route. Detailed descriptions of these models are presented in the sequel

4.1. Material-transfer paths

The first critical issue in modeling a pipeline network should be concerned with system division. In this work, a piping fragment is defined as a collection of pipeline branches and/or processing units separated from other fragments by the valves or other means of flow blockage in the pipeline network (Foulkes, Walton, Andow, & Galluzzo, 1988). Let us consider the P&ID of purifier shown in Fig. 1. Fourteen fragments can be identified, i.e., FR1–FR14, from this flow diagram (see Fig. 6) and the material-transfer paths in different operation periods can be described accordingly (see Table 4). The resulting fragment-based Petri-net model is shown in Fig. 7. The discrete places, FR1–FR14, represent respectively the states of the corresponding piping fragments. Specifically, a token entering such a place denotes the condition that the process fluid is delivered to the corresponding fragment from an upstream source fragment. Thus, the discrete transition between any pair of neighboring places, i.e., MT1–MT14, can be regarded as the corresponding material-transfer actions. Notice that only *one* material-transfer direction is allowed between adjacent fragments in this system. Since the token in place representing a fragment state is immediately removed after firing the transition associated with its outward material-transfer action, the records of flow paths are therefore stored in another set of places RP1–RP14. Finally notice that a material-transfer action can be realized only by opening the valve between it upstream and downstream fragments.

Table 4
Material-transfer paths of process fluids.

Material	Path
C.W.	FR12 → FR13 → FR14
O_2	FR7 → FR2
H_2	FR8 → FR9 → FR3 → FR10 → FR11 FR8 → FR9 → FR4 → FR10 → FR11
N_2	FR1 → FR2 → FR3 → FR5 → FR6 FR1 → FR2 → FR4 → FR5 → FR6

Thus, the places PV(O)s in the aforementioned valve models should be connected to the transitions MT1–MT14 with static test arcs.

It should be noted that more than one exit valve of a fragment may be accidentally kept open at the same time. For the purpose of reducing the possible number of fault propagation scenarios, the corresponding material-transfer actions may be assumed to take place predominantly only in a subset of them and, thus, additional constraints are imposed on the corresponding transitions. For example, fragment FR3 can be connected respectively to its downstream fragment FR10 by opening valve V8 and to FR5 by opening V13. If it can be assumed that the flow resistance in the latter path is much higher than that in the former for the nitrogen flow, transition MT13 should be subject to a set of three additional firing constraints, i.e., V8(+) = V9(+) = RP2 = 1. On the other hand, since the downstream fragments of FR4 are FR5 and FR10, the firing constraints imposed upon transition MT14 should be V10(+) = V11(+) = RP2 = 1. Notice that the firing constraints of transitions MT8, MT9, MT10 and MT11 are stipulated on the basis of the same rationale.

4.2. Input–output models

It is clear from the previous discussions that the piping fragments are defined mainly to facilitate an unambiguous description of all material-transfer paths in the purifier. The operating conditions of each process fluid are altered by the processing units along one of these paths. Notice that a fragment may contain more than one piece of equipment. For example, both adsorber A and pre-heater PH-A are included in fragment FR3 (see Fig. 6). Thus, in order to adequately model the variations in the process conditions along a material-transfer route, it is necessary to further divide every piping fragment into several sub-fragments on the basis of the embedded processing units. Thus, in the case of FR3, two sub-fragments can be identified.

Let us consider the input–output models of the adsorber and pre-heater in FR3 as examples (see Fig. 8). These models are built with discrete transitions, continuous places and normal arcs. Each transition is activated only at a particular state of the corresponding equipment, and its input and output places represent respectively the operating conditions of process fluid in the upstream and downstream sub-fragments. As mentioned previously, the adsor-

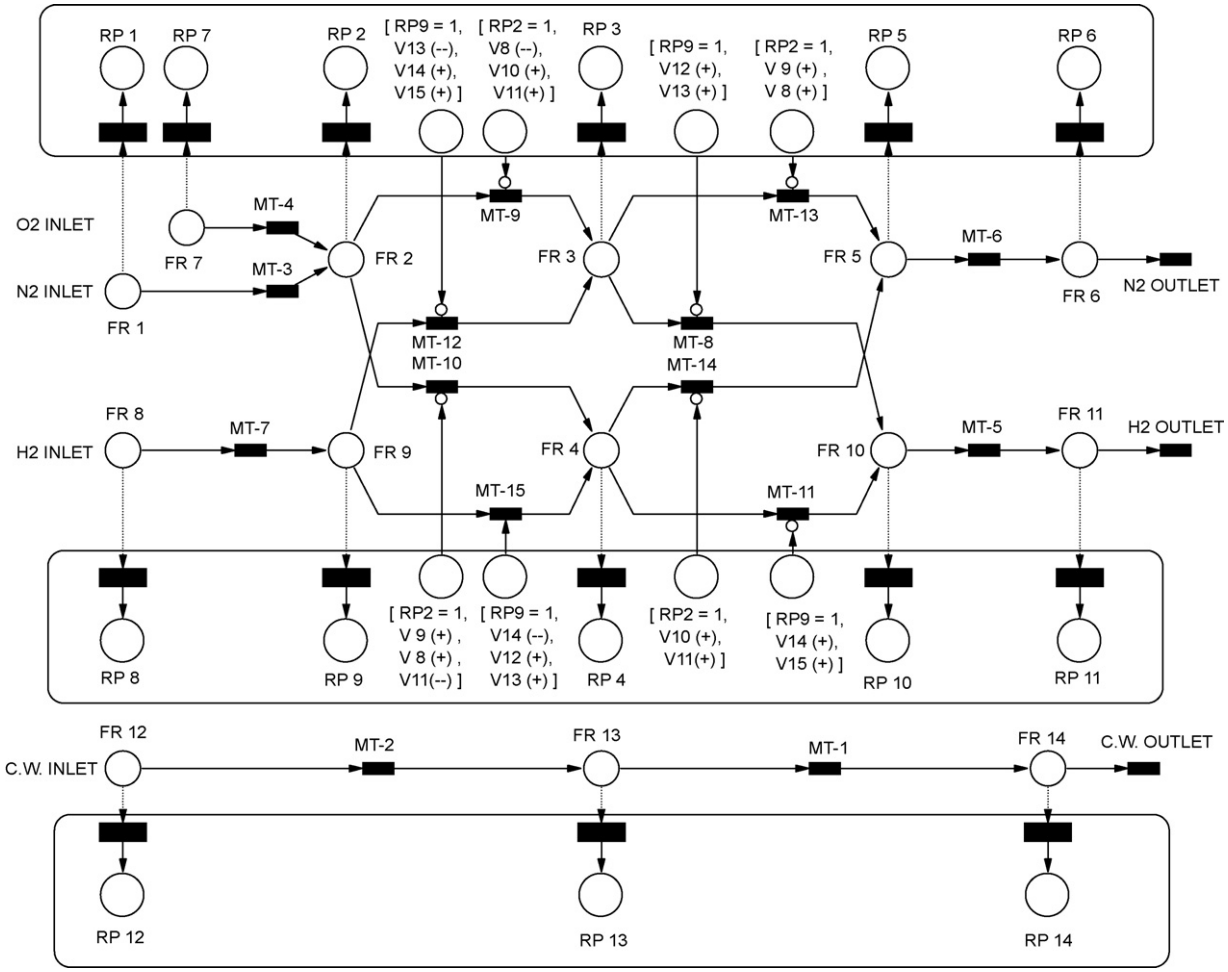

Fig. 7. Fragment-based Petri-net model of pipeline network.

ber states can be characterized by the discrete temperature and saturation levels of adsorbents. In this work, the temperature, flow rate and two impurity concentrations of the process fluid in every sub-fragment are described qualitatively with continuous places labeled with '*T*,' 'F,' 'C1' and 'C2' respectively. In this study, the impurities in the nitrogen stream are classified into two groups: hydrocarbons and others, and C1 and C2 denote the lumped concentrations of these two groups respectively. Since the equipment states are mutually exclusive, at most one transition in an input–output model can be fired at any given time. In this work, three transitions are used to represent the input–output relations at different adsorber states and two used for the pre-heater states. The weight functions on the input and output arcs of each transition are expressed as $f_{i,j}^{\text{in}}$ and $f_{i,j}^{\text{out}}$, where j is the label of a process condition and i that of an equipment state. To keep the token numbers in all continuous places constant during a simulation run, $f_{i,j}^{\text{in}}$ is set to be the token number in the input place of the corresponding normal arc, e.g., $f_{\text{PH-A}(-),F}^{\text{in}} = \langle F3.2 \rangle$. On the other hand, to express the changes in process conditions caused by equipment, the weight functions on the output arcs of the corresponding transition should be assigned as $f_{i,j}^{\text{out}} = a_{i,j} \times f_{i,j}^{\text{in}}$, where the values of parameter $a_{i,j}$ is dependent upon equipment state i and condition j. For example, $a_{\text{PH-A}(+),\text{T}} = 1 + (F_{\text{ref}}/\langle \text{FN3.2} \rangle)$ and $a_{\text{PH-A}(-),\text{T}} = 1$. All weight functions in the input–output models of pre-heater PH-A and adsorber A can be found in Part A of the Supplementary Materials.

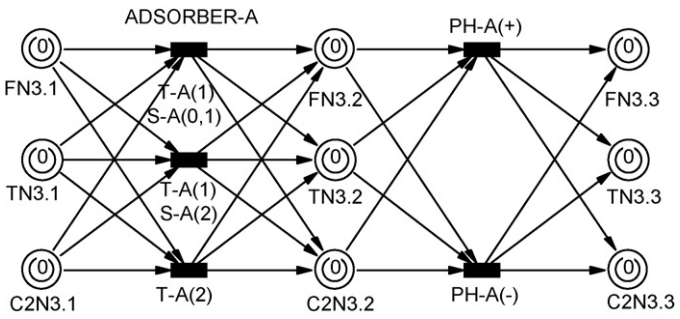

Fig. 8. Input–output model of FR3.

On the other hand, notice that every fragment in this purification system is defined by valves. The structure of input–output model for a valve is essentially the same as those used for the other equipments if it is open. In particular, the weights on the input arcs of the corresponding transition are assigned with the same approach, i.e., each should be identical to the token number in its input place. The weights on the output arcs in this case should all be set to 1, provided that there are no extra material-transfer actions either from the valve's upstream fragment to other downstream fragments and/or from other upstream fragments to the valve's downstream fragment. For example, in the input–output model of valve V5, we can set $a_{\text{V5}(+),\text{T}} = a_{\text{V5}(+),\text{F}} = a_{\text{V5}(+),\text{C1}} = a_{\text{V5}(+),\text{C2}}$. In cases when several different upstream fragments are all connected to the same downstream fragment or the same upstream fragment to several downstream fragments, the weight functions on the out-

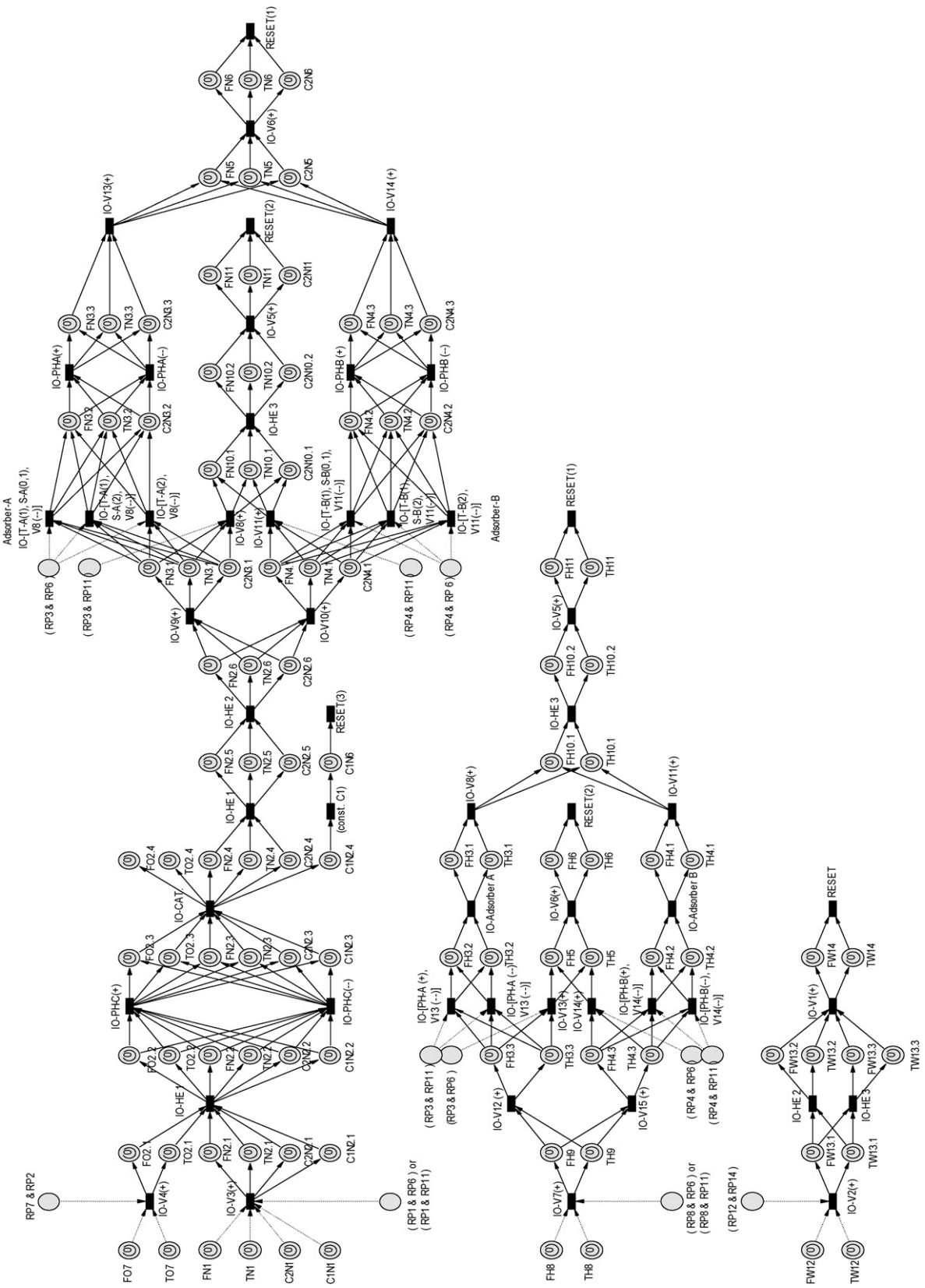

Fig. 9. Disturbance propagation model.

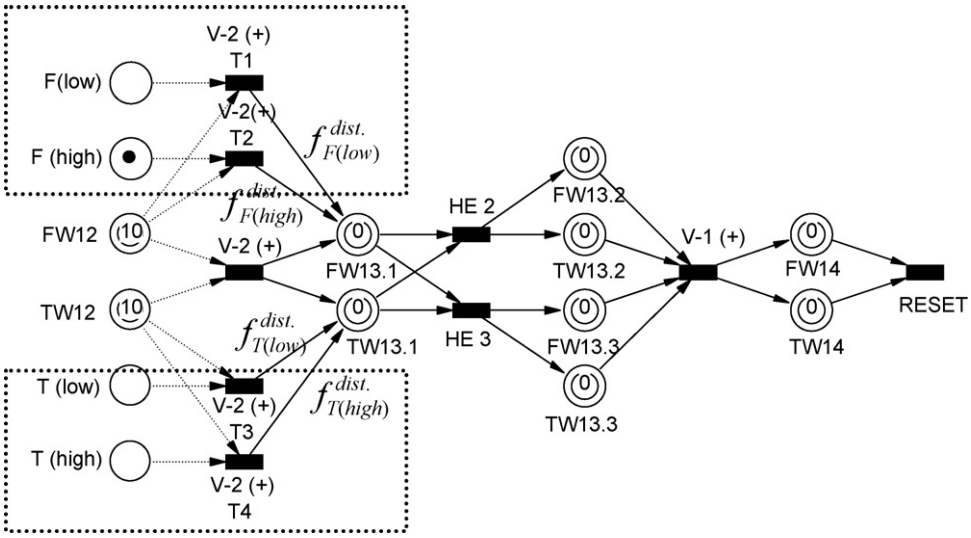

Fig. 10. Disturbance generation mechanism.

put arcs must be assigned on the basis of process considerations. For example, the nitrogen in FR2 flows into either FR3 or FR4 in normal operation, but may flow into both fragments if V9 and V10 are mistakenly kept open at the same time (see Fig. 7). If equal flow rates can be assumed under the latter condition, the parameters of the weight functions on the output arcs of the input–output *flow* models for V9 and V10 should be determined according to the information embedded in path model. More specifically,

$$a_{V9(+),FN}=\begin{cases}1 & \text{if (RP2 = RP3 = 1) and (RP4 = 0) and (RP5 = 1 or RP10 = 1)}\\ 0.5 & \text{if (RP2 = RP3 = RP4 = 1) and (RP5 = 1 or RP10 = 1)}\\ 0 & \text{if otherwise}\end{cases} \quad (8)$$

$$a_{V10(+),FN}=\begin{cases}1 & \text{if (RP2 = RP4 = 1) and (RP3 = 0) and (RP5 = 1 or RP10 = 1)}\\ 0.5 & \text{if (RP2 = RP3 = RP4 = 1) and (RP5 = 1 or RP10 = 1)}\\ 0 & \text{if otherwise}\end{cases} \quad (9)$$

The corresponding temperature and concentration models of V9 and V10 are not affected by this erroneous operation step. On the other hand, notice the process fluid in FR3 and FR4 may meet in FR5 if both V13 and V14 are switched open by mistake. In this situation, the flow rate in FR5 is assumed to be the sum of those in FR3 and FR4, and the other operating conditions (i.e., temperature and impurity concentration) of FR5 are estimated by taking weighted averages of the inlet conditions according to their respective flow rates. Specifically,

$$a_{V13(+),FN} = a_{V14(+),FN} = 1 \quad (10)$$

$$a_{V13(+),TN} = a_{V13(+),C2N} = \frac{\langle FN3.3\rangle}{\langle FN3.3\rangle + \langle V14(+)\rangle\langle FN4.3\rangle} \quad (11)$$

$$a_{V14(+),TN} = a_{V14(+),C2N} = \frac{\langle FN4.3\rangle}{\langle FN4.3\rangle + \langle V13(+)\rangle\langle FN3.3\rangle} \quad (12)$$

The input–output models of all components in the purifier can be constructed with the above principles and then connected according to the P&ID shown in Fig. 1. The corresponding Petri-net model is presented in Fig. 9 and a list of its weight functions can also be found in Supplementary Materials (Part A). Notice that the places representing the process conditions of the source fragments are attached to the Petri net by static test arcs. The implied assumption of this practice is that these conditions are always kept constant during normal operation. On the other hand, notice that each sink place is connected to a transition 'RESET'. This is due to the need to reset the process conditions of the sink fragment and all intermediate sub-fragments to zero if the source fragment is isolated from the other fragments. In this model, the process conditions are allowed to propagate only along an established material-transfer route. Thus, the path records stored in RP1–RP14 are used to impose additional constraints for this purpose. For example, the material-transfer route of nitrogen could be established if this route contains at least a source fragment (which is reflected by a token in PR1) and a sink fragment (which is reflected by a token in PR6 or PR11). Consequently, the firing conditions of the first transition IO-V3(+) in the fault propagation model of the nitrogen system include not only the valve state V3(+) but also the above requirements for an established route.

4.3. Simulation of disturbance propagation behaviors

To facilitate hazard analysis, it is necessary to build additional mechanisms into the system model to simulate the effects of external disturbances. For illustration purpose, let us consider the fault propagation model of the cooling water system, i.e., the third Petri net in Fig. 9, as an example. In Fig. 10, two additional nets, i.e., those enclosed by the dotted lines, are attached to this model. They are used to produce the unexpected changes in the temperature and/or flow rate of cooling water supply. Notice that a disturbance can be introduced by triggering one of the transitions in the dotted boxes. Notice also that, other than the input places, additional firing conditions are also marked. Generally speaking, the prerequisites to initiate a disturbance in the process condition are (1) the isolation valve is open, (2) the source place is not empty, and (3) a token is introduced into the discrete place representing the variable of interest. The changes in the source conditions are specified with the weight functions on arcs between the disturbance-triggering transitions, i.e., T1–T4, and the places representing the process conditions of the downstream fragment of the source. Specifically, they can be written as

$$f^{dist.}_{F(low)} = -\delta \times \langle FW12\rangle \quad (13)$$

$$f^{dist.}_{F(high)} = +\delta \times \langle FW12\rangle \quad (14)$$

$$f^{dist.}_{T(low)} = -\delta \times \langle TW12\rangle \quad (15)$$

$$f^{dist.}_{T(high)} = +\delta \times \langle TW12\rangle \quad (16)$$

where δ is a qualitative measure of the magnitude of disturbance. Let us consider two specific cases in which the source flow rate is perturbed in both positive and negative directions and the magnitudes of both disturbances are characterized as $\delta = 0.6$. In the corresponding simulations runs, it can be found that the token numbers in places representing the flow rates of cooling water, i.e., FW13.1, FW13.2, FW13.3 and FW14, all vary +60% and −60% from their normal levels respectively.

5. Failure models

Other than the external disturbances, abnormal system conditions may also be caused by equipment failures. Thus, it is necessary to incorporate additional elements in each component model to characterize their effects. In general, the direct outcome of a failure can be treated as an abnormal change in the equipment state. This phenomenon can be modeled by disabling a set of normal transitions in the component model and adding another set of alternative transitions. The former task can be achieved with inhibitor arcs and the latter by test arcs. Three typical examples are presented in Fig. 11 concerning (1) the erroneous control actions of PLC, (2) the malfunctions in the two-state components, and (3) the abnormal input–output relations of all components. Following is a brief description of these failure models:

- Two PLC failures are described in Fig. 11(a), i.e., (1) an unnecessary operation step is carried out mistakenly and (2) an essential control step is left out. Notice that the component model for the normal PLC behaviors (Fig. 3) is partially repeated here and, for the sake of clarity, the corresponding failure models are enclosed with dotted line. In the former case, after introducing a token in the discrete place 'MISSING CONTROL SIGNAL', the place representing the operation command 'turn off PH-B' cannot be filled with tokens any more. In the latter failure model, the additional transition can be triggered by inserting a token in the place 'SPURIOUS CONTROL SIGNAL'.
- The Petri net in Fig. 11(b) represents a common failure mechanism of the two-state components, e.g., a valve is stuck or the power of a pre-heater is kept on (or off) permanently. Again, the Petri-net model used for modeling normal operation (Fig. 4) is included here and the failure model is marked with dotted line. The transitions representing the normal state-switching events, i.e., TV(O) and TV(C), are disabled by inserting a token in the place denoting this failure. As a result, this component will remain in its original state indefinitely afterwards.
- The effects of 'pre-heater A fouling' on the output temperature of hydrogen are modeled in Fig. 11(c) with a transition 'IO-PH-A (fouling)' and a place 'FOULING'. Notice that, other than the input places, an additional firing condition is imposed to ensure that this failure takes effect only when the pre-heater is on. The change in the outlet temperature of pre-heater is introduced with the weight function on an outward arc of the fouling–triggering transition. Specifically, this function can be written as $f^{\text{foul}}_{\text{PH-A(+),TH}} = \sigma^{\text{foul}}_{\text{PH-A(+),TH}} \times \langle \text{TH3.3} \rangle$. Notice that any other failure which affects the input–output relation(s) of a component can be modeled with the same approach. Its weight function can be formulated as $f^{\text{failure}}_{i,j} = \sigma^{\text{failure}}_{i,j} \times f^{\text{in}}_{i,j}$, where j is the label of a process condition, i that of an equipment state and $\sigma^{\text{failure}}_{i,j}$ is a qualitative measure of the change caused by the failure. A list of failure models and the corresponding weight functions can also be found in Supplementary Materials (Part B).

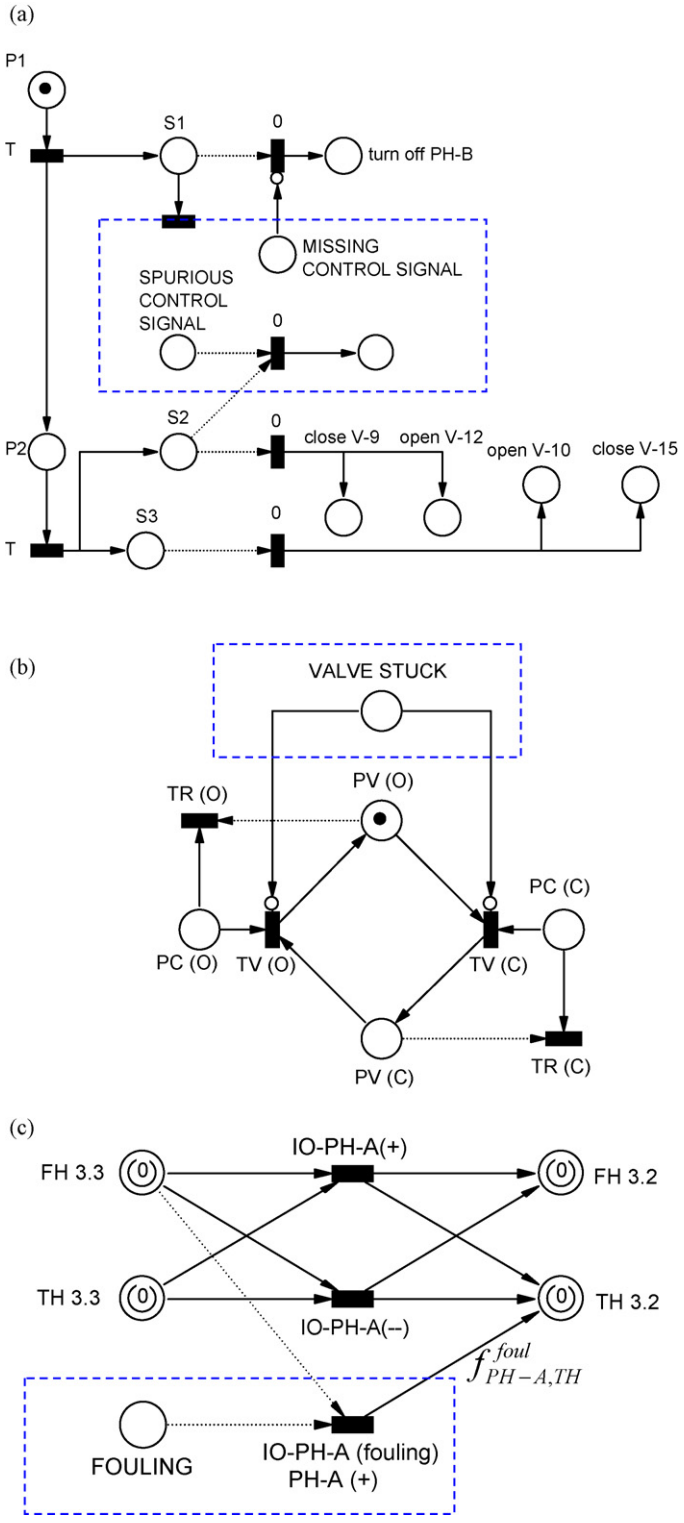

Fig. 11. (a) Failure model of the PLC. (b) Failure model of the valve/pre-heater. (c) Failure model of the pre-heater.

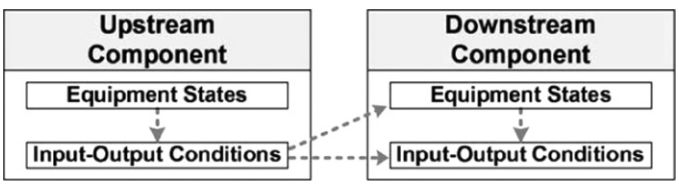

Fig. 12. The connection between two adjacent component models.

Table 5
Effects of an external disturbance.

Disturbance	Disturbance-initiation time	System-failure time	Failure mechanism
FN1 high	Any period	Same period	Exceeding capacities of adsorbers and catalytic bed
TN1 low	Any period	Same period	Low reaction temp in cat. bed
C1N1 high C2N1 high	Any period	Same period	Exceeding capacities of adsorbers and/or catalytic bed
FO7 high	Any period	Same period	Incomplete oxidation in cat. bed
FO7 low	Any period	Same period	Low reaction temp in cat. bed
FH8 low	Period I or II Period III or IV	Period III Next period I	Incomplete regeneration or cooling
TH8 low	Period I Period II or III Period IV	Period III Next period I Next period III	Low regeneration temperature
TH8 high	Period I or II Period III or IV	Period III Next period I	Incomplete cooling
FW12 low TW12 high	Any period	Same period	High N_2 temp at adsorber inlets

6. Hazard analysis

All component models can be combined to form a system model on the basis of the P&ID presented in Fig. 1 and the Grafchart given in Fig. 2. This model construction procedure has already been presented in an earlier paper, e.g., Wang and Chang (2003). Specifically, two adjacent component models can be connected according to Fig. 12. Basically, the output conditions and, in some cases, the equipment states of a downstream component are controlled by the output conditions of an upstream component. The fault propagation behaviors caused by any possible combination of failures and/or disturbances can then be simulated accordingly.

Notice that the process goal of the aforementioned purification operation is obviously to produce the ultra-high purity nitrogen at the specified flow rate and temperature. Thus, this operation should be considered to be failed if, in fragment FR6, at least one of the following conditions can be determined in simulation runs:

- The flow rate of purified nitrogen is too low;
- The impurity concentrations in the nitrogen stream are too high;
- The nitrogen temperature is too high;
- The nitrogen stream is mistakenly replaced by hydrogen.

A large number of simulation studies have been performed with the commercial software VON++ (Drath, 2002) for the purpose of identifying the root causes of these undesirable consequences. To facilitate clear presentation, the simulation results are classified into three groups, i.e., (1) external disturbances, (2) component failures and (3) PLC and two-state equipment failures. The detailed descriptions of these results are presented in the sequel.

6.1. External disturbances

It can be observed from the flow diagram in Fig. 1 that the external disturbances may enter the purification system via four different sources, i.e., the gas supply systems of nitrogen, hydrogen and oxygen, and also the cooling water supply system. Any external disturbance can be introduced during a simulation run with the Petri net described in Fig. 10. In this work, variations in the flow rate, temperature and impurity concentrations of the process fluids from the aforementioned four external sources were considered. The root causes of the designated undesirable consequence "high impurity concentrations in fragment FR6" were then identified from the simulation results. A summary is presented in Table 5. The identified fault origins are presented in the first column. The initiation times of these disturbances and the occurrence times of the aforementioned undesirable consequence (i.e., system-failure times) are given in the second and third columns respectively. Notice that the *disturbance-initiation time* can be "any period", i.e., any one of periods I, II, III and IV, or the specific periods indicated in table. The *system-failure time* can be within

- the "same period" of corresponding disturbance-initiation time,
- "next period I," i.e., period I in the subsequent operation cycle,
- "next period III," i.e., period III in the subsequent operation cycle, or
- "period III," i.e., period III in the current operation cycle.

Finally, brief descriptions of the fault propagation mechanisms are also provided in the last column of the same table.

6.2. Component failures

In this study, simulation runs have also been carried out to confirm if a given component failure could cause the designated undesirable events in purification operation. From the flow diagram in Fig. 1, it can be observed that there are eight process units, i.e., three pre-heaters, two heat exchanges, a catalytic bed, and two adsorption columns. As mentioned previously, a list of typical component failures of these units can be found in Part B of Supplementary Materials. The simulation results of the single-failure scenarios over two consecutive operation cycles are provided in Table 6. Each component failure was introduced respectively during periods I, II, III and IV of the first operation cycle in four separate simulation runs. The failure triggering times are indicated with X's in the table, and the corresponding occurrence times of the designated events are specified respectively with distinct symbols. The definitions of these symbols are given at the bottom of Table 6.

Let us consider the fault propagation scenario resulting from the component failure 'PH-A leak out' as an example. During normal operation, nitrogen passes pre-heater A in periods I and II, and hydrogen passes the same pre-heater in periods III and IV. The flow rate of nitrogen at its exit should decrease once a leak is developed in the first two periods. On the other hand, notice that hydrogen passes pre-heater A during periods III and IV in order to regenerate and then cool down the adsorbent. A leak

Table 6
Effects of a single-component failure.

Equipment failure	Failure triggering and consequence occurrence times							
	I	II	III	IV	I	II	III	IV
PH-A fouling	■				△	△		
		■			△	△		
			■		△	△		
				■				
PH-A leak out	■○	○			○	○△		
		■○			○	○△		
			■		○	○△		
				■	○△	○△		
PH-B fouling	■		△	△			△	△
		■					△	△
			■				△	△
				■			△	△
PH-B leak out	■		○	○△			○	○△
		■	○△	○△			○	○△
			■○	○			○	○△
				■○			○	○△
PH-C fouling	▲	▲	▲	▲	▲	▲	▲	▲
		■▲	▲	▲	▲	▲	▲	▲
			■▲	▲	▲	▲	▲	▲
				■▲	▲	▲	▲	▲
PH-C leak out	■○	○	○	○	○	○	○	○
		■○	○	○	○	○	○	○
			■○	○	○	○	○	○
				■○	○	○	○	○
CAT. BED leak out	■○	○	○	○	○	○	○	○
		■○	○	○	○	○	○	○
			■○	○	○	○	○	○
				■○	○	○	○	○
CAT. BED channeling or non-act.	▲	▲	▲	▲	▲	▲	▲	▲
		■▲	▲	▲	▲	▲	▲	▲
			■▲	▲	▲	▲	▲	▲
				■▲	▲	▲	▲	▲
HE 1 fouling	▲	▲	▲	▲	▲	▲	▲	▲
		■▲	▲	▲	▲	▲	▲	▲
			■▲	▲	▲	▲	▲	▲
				■▲	▲	▲	▲	▲
HE 2 fouling	■◆▲	◆▲	◆▲	◆▲	◆▲	◆▲	◆▲	◆▲
		■◆▲	◆▲	◆▲	◆▲	◆▲	◆▲	◆▲
			■◆▲	◆▲	◆▲	◆▲	◆▲	◆▲
				■◆▲	◆▲	◆▲	◆▲	◆▲
ADSORBER A leak out	■○	○			○	○		
		■○			○	○		
			■		○	○		
				■	○	○		
ADSORBER A Channeling	■△	△			△	△		
		■△			△	△		
			■		△	△		
				■	△	△		
ADSORBER B leak out	■						○	○
		■					○	○
			■○	○			○	○
				■○			○	○
ADSORBER B Channeling	■		△	△			△	△
		■	△	△			△	△
			■△	△			△	△
				■△			△	△

(■) Triggering time of component failure; (▲) high impurity concentration, i.e., C1N6(+); (△) high impurity concentration, i.e., C2N6(+); (◆) high nitrogen temperature, i.e., TN6(+); (○) low nitrogen flow rate, i.e., FN6(−).

in the pre-heater during period III could reduce hydrogen flow and consequently hamper the regeneration efficiency. However, since the adsorbent is not sufficiently heated in period III, the column temperature could be cooled to its normal level with the reduced hydrogen flow in period IV. Thus, if the adsorbed impurities are only partially removed after the completion of cycle 1, then it is conceivable that the adsorbent will be saturated in only one period in the next cycle. As a result, the impurity concentration in the nitrogen stream at the exit of purifier will be too high in the following period II. Finally, if the leak occurs in period IV, then obviously the column temperature cannot be cooled to its normal level by the end of the first cycle. Thus, the adsorbent becomes too hot for adsorption operation in period I of the second cycle, and the undesirable condition of high impurity concentration in the exit nitrogen stream could appear during this period.

6.3. PLC and two-state equipment failures

From the Grafchart shown in Fig. 2, it can be observed that the process configuration of the purifier is altered from period to period by manipulating the valves and pre-heaters, and these two-state equipments are in turn controlled by the PLC. In this study, the adverse effects of abnormal process configurations, which can be attributed to malfunctions in the above equipments, have also been simulated for the purpose of hazard identification.

Table 7
Effects of a single PLC failure.

No.	Spurious PLC action			Consequence occurrence time							
	Affected equipment	Erroneous state	Triggering time	I	II	III	IV	I	II	III	IV
1	PH-B	+	I–II			△ ♦	△ ♦				
		+	II–III			♦	♦				
		+	III–IV				♦				
		–	IV–I							△	△
2	PH-A	+	I–II		♦						
		–	II–III					△	△		
		+	III–IV					△ ♦	△ ♦		
		+	IV–I					♦	♦		
3	V8	+	I–II		○						
		–	II–III					△	△		
		–	III–IV						△		
		+	IV–I					○	○		
4	V9	–	I–II		○						
		+	II–III			○	○				
		+	III–IV				○				
		–	IV–I					○	○		
5	V10	+	I–II		○						
		–	II–III			○	○				
		–	III–IV				○				
		+	IV–I					○	○		
6	V11	–	I–II				△				
		+	II–III			○	○				
		+	III–IV				○				
		–	IV–I							△	△
7	V12	+	I–II		●		△				
		–	II–III					△	△		
		–	III–IV						△		
		+	IV–I					●	●	△	△
8	V13	–	I–II		○						
		+	II–III			●	●	△	△		
		+	III–IV				●		△		
		–	IV–I					○	○		
9	V14	+	I–II		●		△				
		–	II–III			○	○				
		–	III–IV				○				
		+	IV–I					●	●	△	△
10	V15	–	I–II				△				
		+	II–III			●	●	△	△		
		+	III–IV				●		△		
		–	IV–I							△	△

(▲) high impurity concentration, i.e., C1N6(+); (△) high impurity concentration, i.e., C2N6(+); (♦) high nitrogen temperature, i.e., TN6(+); (○) low nitrogen flow rate, i.e., FN6(–); (●) exported flow rate of hydrogen is failing high, i.e., FH6(+).

A PLC failure mode can be described according to Fig. 11(a) by inserting a spurious control command just after the controller issues the routine one(s) at the transition time between two successive periods. The simulation results of the single-failure scenarios over two consecutive operation cycles can be found in Table 7. Since, in each scenario, a valve or a pre-heater is directly affected by the erroneous PLC action, this equipment and its state are listed in columns 2 and 3 respectively. The failure triggering times are given in the fourth column in the table, and the corresponding occurrence times of the designated events are specified respectively with four distinct symbols. The definitions of these symbols are the same as those given in Table 6.

On the other hand, only the failure mode "sticking" is included in every two-state equipment model. This model can be constructed according to Fig. 11(b). The simulation results of the corresponding single-failure scenarios over three consecutive operation cycles are presented in Table 8. Each failure was introduced repeatedly in the beginning of every period during the first operation cycle. The failure triggering times are listed in the third column in the table, and the corresponding occurrence times of the designated undesirable events are specified respectively with the same symbols defined before.

The multi-failure scenarios have also been studied extensively. Due to the limitation of space, only the simulation results of *one* two-failure case study are described here. Let us consider, as an example, the effects of following two initiating events: (1) an additional erroneous PLC signal issued to V8 at the instance between periods IV and I, and (2) V8 itself then sticks during period II. Normally, valve V8 is closed between periods IV and I, and open between periods II and III for the purpose of removing hydrogen from adsorber A. The above-mentioned failures cause V8 to remain open permanently after the 2nd period of the first cycle. According to the assumptions given in Section 4.1, nitrogen stream should pass through valves V9 and V8 directly when both are open. Thus, this stream should also leave the purifier via fragment FR10

Table 8
Effects of a single two-state equipment failure.

No.	Equipment sticking		Consequence occurrence time											
	Component	Triggering time	I	II	III	IV	I	II	III	IV	I	II	III	IV
1	V8	I					△	△			△	△		
		II					△	△			△	△		
		III					○	○			○	○		
		IV					○	○			○	○		
2	V9	I			○	○			○	○			○	○
		II			○	○			○	○			○	○
		III					○	○			○	○		
		IV					○	○			○	○		
3	V10	I			○	○			○	○			○	○
		II			○	○			○	○			○	○
		III					○	○			○	○		
		IV					○	○			○	○		
4	V11	I			○	○			○	○			○	○
		II			○	○			○	○			○	○
		III							△	△			△	△
		IV							△	△			△	△
5	V12	I					△	△			△	△		
		II					△	△			△	△		
		III					●	●	△	△	●	●	△	△
		IV					●	●	△	△	●	●	△	△
6	V13	I			●	●	△	△	●	●	△	△	●	●
		II			●	●	△	△	●	●	△	△	●	●
		III					○	○			○	○		
		IV					○	○			○	○		
7	V14	I			○	○			○	○				
		II			○	○			○	○				
		III					●	●	△	△	●	●	△	△
		IV					●	●	△	△	●	●	△	△
8	V15	I			●	●	△	△	●	●	△	△	●	●
		II			●	●	△	△	●	●	△	△	●	●
		III							△	△			△	△
		IV							△	△			△	△
9	PH-A	I					△	△			△	△		
		II					△	△			△	△		
		III					♦	♦			♦	♦		
		IV									△	△		
10	PH-B	I			♦	♦			♦	♦			♦	♦
		II							△	△			△	△
		III							△	△			△	△
		IV							△	△			△	△

(▲) high impurity concentration, i.e., C1N6(+); (△) high impurity concentration, i.e., C2N6(+); (♦) high nitrogen temperature, i.e., TN6(+); (○) low nitrogen flow rate, i.e., FN6(−); (●) exported flow rate of hydrogen is failing high, i.e., FH6(+).

together with the hydrogen coming from adsorption column B in periods I and II in every cycle afterwards. As a result, the flow rate of purified nitrogen stream in FN6 should be very low (or zero) in these periods.

7. Conclusions

A hierarchical approach is proposed in this study to construct a Petri-net model for the purification operation in MOCVD process. Simple simulation techniques are presented to predict the effects of a given set of component failures and/or external disturbances. By following the proposed method, reasonable prediction and comprehensive enumeration of the critical effects produced in various fault propagation scenarios can be carried out systematically. It is clear from the application results that the proposed Petri-net models can also be used as the basis for efficient hazard identification in other semiconductor manufacturing processes as well.

Acknowledgement

This work is supported by the National Science Council of the ROC Government under Grant NSC91-2214-E-006-01.

Appendix A. A brief review of the ordinary Petri net and its extensions

A formal mathematical description of the ordinary Petri net can be found in Peterson (1981). For the sake of brevity, only a condensed version is provided here. As originally designed, the *ordinary* Petri net consists of only three types of elements, i.e., places, transitions and arcs. The state of a discrete-event system is basically reflected with a *marking*, i.e., a vector of the *token* numbers in all places of the Petri-net model. Since only the discrete places are considered in the ordinary Petri net, this vector contains only positive integers and/or zeros. The movements of tokens can be realized by *enabling* and then immediately *firing* the transitions. A transition is

Table A.1
The transition enabling rules.

Arc type	Enabling condition	Token removal from input place
Normal arc	$M \geq W$	Yes
Static test arc	$M \geq W$	No
Inhibitor arc	$M < W$	No

enabled if the token number in every input place is larger than or equal to the *weight* on the corresponding place-to-transition arc. After firing the transition, additional tokens are introduced into its output places and the increased token number in each place is the weight on the corresponding transition-to-place arc. Finally, it should be noted that the only allowed weight in an ordinary Petri net is 1 and all the transitions are without time delay.

In order to facilitate proper representation of realistic operations, several special extensions have been adopted in this study (Alla & David, 1998; Bowden, 2000; David & Alla, 1994; Drath, 1998). Following is a list of specific places and transitions used in the proposed Petri-net models.

A.1. The discrete and continuous places

Both the *discrete* and *continuous* places are adopted in this work. A discrete place can be used to represent the Boolean state of a device, e.g., the open/close position of a valve or the on/off status of a power supply. On the other hand, since the token number in a continuous place is real, it is well suited for describing the variation of a state variable, such as the temperature, pressure or liquid level, associated with a process unit.

A.2. The timed and non-timed transitions

Both the timed and non-timed transitions are used in the proposed system models. It should be noted that various events can take place over a wide range of different time spans in sequential operations. The non-timed transitions are suitable for representing events occurring almost instantly. There are in general two alternative mechanisms for representing nonzero event times. They can be either associated with the places (P-timed) or with the transitions (T-timed). Since it is always possible to transform from a P-timed Petri net to a T-timed Petri net, and vice versa, the latter is chosen in this work.

In addition, three different types of place-to-transition arcs are utilized, i.e., the weighted arcs, the inhibitor arcs and the static test arcs. The transition enabling rules of these place-to-transition arcs are listed in Table A.1. In this table, M denotes the number of tokens in input places and W denotes the weight of corresponding arc.

Note that a time-delayed transition cannot be fired right after the enabling condition is satisfied. Extra tokens will not be added in its output places until the designated firing duration has elapsed. Additional details concerning these arcs are summarized below.

A.3. The weighted arcs

A generalized version of the arcs in an ordinary Petri net is one in which the arc weight may not be one. A positive integer k can be used to label the outward arc of a discrete place. A k-weighted arc can be interpreted as a set of k parallel arcs. For the sake of simplicity, the unity weights are omitted. On the other hand, if an arc is attached to a continuous place, one can use a mathematical function of the token numbers in a set of selected places as the weight.

A.4. The inhibitor arcs

An inhibitor arc is usually represented by a directed arc with a small circle at its end. The token number in its input place remains unchanged even after firing the output transition. This type of arcs can be used in executing zero test or in modeling the failure mechanisms that inhibit certain normal events in operation.

A.5. The static test arcs

The static test arc is marked by a directed dash line. In general, it is often used to replace the self-looping structure in Petri net. In other words, a static test arc is equivalent to two equally weighted arcs pointing in opposite directions. Notice that this arc also does not allow token flow, i.e., the token quantity of its input place cannot be reduced by firing the output transition.

Finally, it should be noted that all transition-to-place arcs are weighted arcs. If an arc is directed toward a continuous place and a mathematical function is used as its weight, the independent variables of this function should be the token numbers in selected places.

Appendix B. Supplementary data

Supplementary data associated with this article can be found, in the online version, at doi:10.1016/j.compchemeng.2010.05.006.

References

Alla, H., & David, R. (1998). A modeling and analysis tool for discrete events systems: Continuous Petri net. *Performance Evaluation*, *33*, 175.

Allen, D. J., & Rao, M. S. M. (1980). New algorithms for the synthesis and analysis of fault trees. *Industrial and Engineering Chemistry Fundamentals*, *19*, 79.

Andrews, J. D., & Morgan, J. M. (1986). Application of digraph method of fault tree construction to process plant. *Reliability Engineering and System Safety*, *14*, 85.

Balasubramanian, N., Chang, C. T., & Wang, Y. F. (2002). Petri-net models for risk analysis of hazardous liquid loading operations. *Industrial and Engineering Chemistry Research*, *41*, 4823.

Bowden, F. D. J. (2000). A brief survey and synthesis of the roles of time in Petri nets. *Mathematical and Computer Modelling*, *31*, 55.

Cavalieri, S., Mirabella, O., & Marroccia, S. (1997). Improving flexible semiconductor manufacturing system performance by a coloured Petri net-based scheduling algorithm. In *Proceedings of IEEE sixth international conference on emerging technologies and factory automation* (p. 369).

Chang, C. T., Hsu, D. S., & Hwang, D. M. (1994). Studies on the digraph-based approach for fault-tree synthesis. 2. The trip systems. *Industrial and Engineering Chemistry Research*, *33*, 1700.

Chang, C. T., & Hwang, H. C. (1992). New development of the digraph-based techniques for fault-tree synthesis. *Industrial and Engineering Chemistry Research*, *32*, 1490.

Chang, C. T., & Hwang, H. C. (1994). Studies on the digraph-based approach for fault-tree synthesis. 1. The ratio-control systems. *Industrial and Engineering Chemistry Research*, *33*, 1520.

David, R., & Alla, H. (1994). Petri net for modeling of dynamic systems—A survey. *Automatica*, *30*, 175.

Drath, R. (1998). Hybrid object nets: An object oriented concept for modeling complex hybrid systems. In *Proceedings of 3rd international conference on automation of mixed processes: Hybrid dynamical systems* (p. 437).

Drath, R. (2002). *Visual object net ++, Version 2.7a*. Paramsoft Software Development.

Foulkes, N. R., Walton, M. J., Andow, P. K., & Galluzzo, M. (1988). Computer-aided synthesis of complex pump and valve operations. *Computers and Chemical Engineering*, *12*, 1035.

Jones, A. C., & O'Brien, P. (1996). *CVD of compound semiconductors*. Weinheim: VCH.

Kelly, B. E., & Lees, F. P. (1986a). The propagation of faults in process plants. 1. Modeling of fault propagation. *Reliability Engineering and System Safety*, *16*, 3.

Kelly, B. E., & Lees, F. P. (1986b). The propagation of faults in process plants. 2. Fault tree synthesis. *Reliable Engineering and System Safety*, *16*, 39.

Kim, J., & Desrochers, A. A. (1997). Modeling and analysis of semiconductor manufacturing plants using time Petri net models: COT business case study. In *IEEE international conference on systems, man, and cybernetics, Vol. 4* (p. 3227).

Kumamoto, H., & Henley, E. J. (1979). Safety and reliability synthesis of systems with control loops. *AIChE Journal*, *20*, 376.

Lapp, S. A., & Powers, G. J. (1977). Computer-aided synthesis of fault trees. *IEEE Transaction on Reliability*, *R-26*, 2.

McCoy, S. A., Wakeman, S. J., Larkin, F. D., Chung, P. W. H., Rushton, A. G., & Lees, F. P. (1999). HAZID, a computer aid for hazard identification. 2. Unit model system. *Transactions of the Institution of Chemical Engineers, Part B (Process Safety and Environmental Protection)*, *77*, 328.

McCoy, S. A., Wakeman, S. J., Larkin, F. D., Chung, P. W. H., Rushton, A. G., Lees, F. P., et al. (1999). HAZID, a computer aid for hazard identification. 3. The fluid model and consequence evaluation systems. *Transactions of the Institution of Chemical Engineers, Part B (Process Safety and Environmental Protection)*, *77*, 335.

McCoy, S. A., Wakeman, S. J., Larkin, F. D., Chung, P. W. H., Rushton, A. G., & Lees, F. P. (2000a). HAZID, a computer aid for hazard identification. 4. Learning set, main study system, output quality and validation trials. *Transactions of the Institution of Chemical Engineers, Part B (Process Safety and Environmental Protection)*, *78*, 91.

McCoy, S. A., Wakeman, S. J., Larkin, F. D., Chung, P. W. H., Rushton, A. G., & Lees, F. P. (2000b). HAZID, a computer aid for hazard identification. 5. Future development topics and conclusions. *Transactions of the Institution of Chemical Engineers, Part B (Process Safety and Environmental Protection)*, *78*, 120.

McCoy, S. A., Wakeman, S. J., Larkin, F. D., Jefferson, M. L., Chung, P. W. H., Rushton, A. G., et al. (1999). HAZID, a computer aid for hazard identification. 1. The STOP-HAZ package and the HAZID code: An overview, the issues and the structure. *Transactions of the Institution of Chemical Engineers, Part B (Process Safety and Environmental Protection)*, *77*, 317.

Newey, J. (2001). Gas purifiers earn their place in MOCVD material growth. *Compound Semiconductor*, *12*, 51.

Peterson, J. L. (1981). *Petri net theory and the modeling of systems*. Englewood Cliffs, NJ: Prentico-Hall.

Petri, C. A. (1962). *Kommunikation mit Automaten*. Ph.D. thesis, University of Bonn, Bonn, Germany.

Rossing, N. L., Lind, M., Jensen, N., & Jorgensen, S. B. (2010). A functional HAZOP methodology. *Computers and Chemical Engineering*, *34*, 244.

Sangwal, K. (1996). Effects of impurities on crystal growth processes. *Progress in Crystal Growth and Characterization of Materials*, *32*, 3.

Srinivasan, R., & Venkatasubramanian, V. (1998a). Automating HAZOP analysis of batch chemical plants. Part I. The knowledge representation framework. *Computers and Chemical Engineering*, *22*, 1345.

Srinivasan, R., & Venkatasubramanian, V. (1998b). Automating HAZOP analysis of batch chemical plants. Part II. Algorithms and application. *Computers and Chemical Engineering*, *22*, 1357.

Stringfellow, G. B. (1989). *Organometallic vapor-phase epitaxy*. New York: Academic Press.

Stringfellow, G. B. (1994). *Handbook of crystal growth* Amsterdam: Elsevier Science.

Szucs, A., Gerzson, M., & Hangos, K. (1998). An intelligent diagnostic system based on Petri nets. *Computers and Chemical Engineering*, *22*, 1335.

Thompson, A. G. (1997). MOCVD technology for semiconductors. *Materials Letters*, *30*, 255.

Vaidhyanathan, R., & Venkatasubramanian, V. (1995). Digraph-based models for automated HAZOP analysis. *Reliability Engineering and System Safety*, *50*, 33.

Vaidhyanathan, R., & Venkatasubramanian, V. (1996a). Haxop expert: An expert system for automating HAZOP analysis. *Process Safety Progress*, *15*, 80.

Vaidhyanathan, R., & Venkatasubramanian, V. (1996b). A semi-quantitative reasoning methodology for filtering and ranking HAZOP results in HAZOP expert. *Reliability Engineering and System Safety*, *53*, 185.

Veintemillas-Verdaguer, S. (1996). Chemical aspects of the effect of impurities in crystal growth. *Progress in Crystal Growth and Characterization of Materials*, *32*, 3.

Wang, Y. F., & Chang, C. T. (2003). A hierarchical approach to construct Petri nets for modeling the fault propagation mechanisms in sequential operations. *Computers and Chemical Engineering*, *27*, 259.

Wang, Y. F., & Chang, C. T. (2004). Petri-net-based deductive reasoning strategy for fault identification in batch processes. *Industrial and Engineering Chemistry Research*, *43*, 2704.

Wang, Y. F., Wu, J. Y., & Chang, C. T. (2002). Automatic hazard analysis of batch operations with Petri nets. *Reliability Engineering and System Safety*, *76*, 91.

Watanabe, T., Funke, H. H., Torres, R., Raynor, M. W., Vininski, J., & Houlding, V. H. (2003). Contamination control in gas delivery systems for MOCVD. *Journal of Crystal Growth*, *248*, 67.

Zhao, C., Bushan, M., & Venkatasubramanian, V. (2005a). PHASuite: An automated HAZOP analysis tool for chemical processes. Part I. Knowledge engineering framework. *Transactions of the Institution of Chemical Engineers, Part B (Process Safety and Environmental Protection)*, *83*, 509.

Zhao, C., Bushan, M., & Venkatasubramanian, V. (2005b). PHASuite: An automated HAZOP analysis tool for chemical processes. Part II. Implementation and case study. *Transactions of the Institution of Chemical Engineers, Part B (Process Safety and Environmental Protection)*, *83*, 533.